Molecular and Meso- and Macroscopic Properties of Hierarchical Nanocrystalline ZSM-5 Zeolite Prepared by Seed Silanization

D. P. Serrano,*[,†,‡] J. Aguado,[†] G. Morales,[†] J. M. Rodríguez,[†] A. Peral,[†] M. Thommes,[§] J. D. Epping,[||] and B. F. Chmelka[||]

Department of Chemical and Environmental Technology, ESCET, Rey Juan Carlos University, Móstoles 28933, Spain, Madrid Institute for Advanced Studies on Energy, IMDEA Energía, Móstoles 28933, Spain, Quantachrome Instruments, 1900 Corporate Drive, Boynton Beach, Florida 33426, and Department of Chemical Engineering, University of California, Santa Barbara, California 93106

Received July 17, 2008. Revised Manuscript Received December 19, 2008

Surface-passivating silanization of protozeolitic units has been shown to be an effective strategy for the preparation of ZSM-5 nanocrystals, showing a controlled aggregation degree and a hierarchical porosity. ZSM-5 zeolite materials are thus obtained with adjustable and relatively uniform mesoporosities that have a strong influence on resulting macroscopic reaction properties, especially for macromolecular reagents. The mean sizes of the nanounits and, therefore, the textural and accessibility of these materials can be varied by changing the precrystallization conditions and the concentration of the seed-silanization agent. In addition to conventional characterization techniques, solid-state two-dimensional (2D) nuclear magnetic resonance (NMR) spectroscopy measurements and the application of the NLDFT model to the argon adsorption isotherms have allowed both the local and the mesoscopic compositions, as well as the structures of the hierarchically porous ZSM-5 materials, to be established. The resulting combination of mesopore sizes and exterior-nanocrystal surface properties of the hierarchically structured ZSM-5 zeolites is shown to catalyze reactions that are otherwise limited by steric and/or diffusional limitations, as demonstrated by their enhanced activity for polyethylene cracking.

1. Introduction

Zeolites are crystalline aluminosilicates that possess uniform subnanometer-size pores and cavities with dimensions that are close to those of numerous molecular species of high commercial interest. Accordingly, zeolites are known to exhibit molecular sieve and shape-selective properties, based on the diffusional access of guest species into their subnanometer-size pores and associated shapes.[1] As a result of their crystalline nature, zeolites exhibit high thermal and hydrothermal stabilities. Moreover, zeolites may incorporate a large number of heteroatoms in four-coordinated sites in the crystalline lattice and may also be used as supports for dispersed metals and metal oxides, conferring these materials with catalytic properties for a large variety of reactions. As a consequence, zeolites are solids with significant industrial applications as catalysts, adsorbents, and ion exchangers.

For many years, it has been considered that the presence of active sites on the external surfaces of zeolite crystals can have a detrimental effect on their overall catalytic properties, because their accessibility tends to allow transformations that are not size or shape selective.[2] Accordingly, zeolites have usually been synthesized with crystal sizes in the micrometer range, and therefore, with negligible external surface areas. Moreover, a number of methods were developed in the past for the removal or passivation of the active sites on the external surface of the zeolite particles to ensure high shape-selectivities when used as catalysts.[2,3]

Recently, however, there has been increasing interest in the synthesis, characterization, and properties of nanocrystalline zeolites having crystal sizes below 100 nm.[4−6] In these materials, the external surface area can no longer be considered negligible and, on the contrary, it becomes an essential factor that imparts significantly different adsorption and reaction properties, compared to bulk zeolite crystals, which may enable a number of new applications.[7] In spite of their inherently lower shape-selectivity, a number of advantages can be derived from nanozeolite catalysts: the active sites on the external surfaces may catalyze reactions involving large molecules, while the decrease in the crystal size reduces intracrystalline diffusional limitations. Likewise, it has been suggested that the deactivating effect caused by coke deposits is less pronounced when using zeolite nanocrystals.[8]

In the search for zeolitic materials capable of catalyzing reactions involving large molecules, different achievements

* Corresponding author. E-mail: david.serrano@urjc.es.
† Rey Juan Carlos University.
‡ IMDEA Energía.
§ Quantachrome Instruments.
|| University of California.

(1) Corma, A. *J. Catal.* **2003**, *216* (1−2), 298.
(2) Uguina, M. A.; Sotelo, J. L.; Serrano, D. P.; Van Grieken, R. *Ind. Eng. Chem. Res.* **1992**, *31* (8), 1875.
(3) Weber, R. W.; Fletcher, I. C. Q.; Moller, K. P.; O'Connor, C. T. *Microporous Mater.* **1996**, *7* (1), 15.
(4) Tosheva, L.; Valtchev, V. P. *Chem. Mater.* **2005**, *17*, 2494.
(5) Karami, D.; Rohani, S. *Rev. Chem. Eng.* **2007**, *23* (1), 1.
(6) Song, W.; Justice, R. E.; Jones, C. A.; Grassian, V. H.; Larsen, S. C. *Langmuir* **2004**, *20* (19), 8301.
(7) Larsen, S. C. *J. Phys. Chem. C* **2007**, *111* (50), 18464.
(8) Hsu, Ch.-Y.; Chiang, A. S. T.; Selvin, R.; Thompson, R. W. *J. Phys. Chem. B* **2005**, *109*, 18804.

10.1021/cm801951a CCC: $40.75
Published on Web 01/28/2009

have been recently reported.[9] These include syntheses within and/or around carbon matrices,[10,11] the generation of a secondary mesoporosity by steaming (dealumination),[12] treatment under basic conditions (desilication),[13,14] templating by silane-functionalized polymers,[15] steam zeolitization of surfactant-protected zeolite precursors,[16] the synthesis of hybrid ordered mesoporous materials with zeolitic walls,[17,18] the preparation of delaminated zeolites,[19] and the synthesis of colloidal zoned MFI crystals, that is, continuous crystals with a compositional gradient resulting in a ZSM-5 core covered with a silicalite-1 shell.[20] In the last three approaches, surfactant molecules are used to prevent aggregation of growing zeolite crystallites, to promote the assembly of the zeolite seeds into mesostructured frameworks, or to induce the delamination of a layered precursor, respectively. Likewise, it has been recently reported how the use of an amphiphilic organosilane surfactant leads to the synthesis of crystalline zeolites with adjustable mesoporosities.[21]

While extensive efforts have been made to prepare colloidal and nanocrystalline silicalite-1 (a purely siliceous zeolite with the MFI structure),[22,23] reports on the synthesis and properties of nanosized aluminosilicate ZSM-5, which shares the MFI topology, are scarce.[24] The direct synthesis of nanocrystalline MFI materials is usually based on crystallization conditions that lead to high nucleation rates, namely, high concentrations of the silica source, strong basicity, and the absence of alkali cations.[23] Recently, low temperature methods have been developed for the synthesis of ZSM-5 formed by aggregates of 20−40 nm nanocrystals.[25] However, under these conditions, the crystallization proceeds with low synthesis yields and, in many cases, the zeolite product may be contaminated by the presence of an amorphous phase.

The synthesis of organofunctionalized molecular sieves (OFMSs) by incorporation of organic moieties into the synthesis gel was first reported by Davis et al.[26] In this case, the organosilane species were added to a synthesis mixture of zeolite Beta as an additional silica source, being incorporated within the zeolite nanopores, as evidenced by the observed loss of adsorption capacity of the functionalized zeolite. Recently, hybrid zeolites containing organic methylene groups in framework positions have been crystallized from gels with bis(triethoxysilyl) methane partially substituting the silica source.[27]

In a previous communication,[28] we introduced a novel strategy for the synthesis of hierarchical nanozeolites, based on the use of organosilanes to prevent zeolite crystal growth, and thereby to stabilize zeolitic particles with ultrasmall sizes. The final hydrothermal crystallization treatment occurs at relatively high temperature, thus making compatible the preparation of ultrasmall nanocrystals also with high zeolite synthesis yields. In a subsequent work, the effect of the silanization agent nature on the synthesis of hierarchical nanocrystalline ZSM-5 has been investigated, the best results being obtained with phenylaminopropyl−trimethoxysilane (PHAPTMS).[29] Moreover, we have shown that this strategy can be generally applicable to the syntheses of other zeolites with enhanced textural features, hierarchical porosities, and significantly improved catalytic properties, as it is the case of zeolite Beta or mordenite.[30,31]

In the present work, we report the effect of two synthesis parameters (precrystallization temperature and proportion of silanization agent) that allow the hierarchical features of the nanocrystalline ZSM-5 to be varied and controlled. Moreover, the use of advanced techniques, such as solid-state two-dimensional (2D) nuclear magnetic resonance (NMR) spectroscopy and the application of the NLDFT model to the argon adsorption isotherms, have provided essential insights on the synthesis mechanisms, as well as on the molecular, mesostructural, and macroscopic properties of nanocrystalline zeolite ZSM-5 with hierarchical porosities and significantly enhanced catalytic activity in the conversion of bulky compounds.

2. Experimental Section

Precursor ZSM-5 zeolite solutions were prepared with the following molar composition: 1 Al_2O_3:60 SiO_2:11 TPAOH:1500 H_2O. Tetraethoxysilane (TEOS, 98%; Aldrich), tetrapropylammonium hydroxide (TPAOH, 40%; Alfa), aluminum isopropoxide (AIP; Aldrich), and distilled water were used as starting materials. The clear precursor solutions were precrystallized under reflux with stirring (100 rpm) at 40 °C (low temperature precrystallization, LTP) or 90 °C (high temperature precrystallization, HTP) for 20 h. The resulting zeolite seeds were then functionalized by reaction with phenylaminopropyltrimethoxysilane (PHAPTMS; Aldrich) at 90 °C

(9) Tao, Y.; Kanoh, H.; Abrams, L.; Kaneko, K. *Chem. Rev.* **2006**, *106*, 896.
(10) Jacobsen, C. J. H.; Madsen, C.; Houzvicka, J.; Schmidt, I.; Carlsson, A. *J. Am. Chem. Soc.* **2000**, *122*, 7116.
(11) Yang, Z.; Xia, Y.; Mokaya, R. *Adv. Mater.* **2004**, *16* (8), 727.
(12) van Dok, S.; Janssen, A. H.; Bitter, J. H.; de Jong, K. P. *Catal. Rev.* **2003**, *45* (2), 297.
(13) Groen, J. C.; Moulijn, J. A.; Pérez-Ramírez, J. *J. Mater. Chem.* **2006**, *16*, 2121.
(14) Groen, J. C.; Peffer, L. A. A.; Moulijn, J. A.; Pérez-Ramírez, J. *Chem. Eur. J.* **2005**, *11*, 4983.
(15) Wang, H.; Pinnavaia, T. J. *Angew. Chem., Int. Ed.* **2006**, *45*, 7603.
(16) Naik, S. P.; Chen, J. C.; Chiang, A. S. T. *Microporous Mesoporous Mater.* **2002**, *54*, 293.
(17) Liu, Y.; Zhang, W.; Pinnavaia, T. J. *J. Am. Chem. Soc.* **2000**, *122*, 8791.
(18) Han, Y.; Wu, S.; Sun, Y.; Li, D.; Xiao, F. S.; Liu, J.; Zhang, X. *Chem. Mater.* **2002**, *14*, 1144.
(19) Corma, A.; Fornés, V.; Pergher, S. B.; Maesen, Th.L.M.; Buglass, J. G. *Nature* **1998**, *396*, 353.
(20) Li, Q.; Wang, Z.; Hedlund, J.; Creaser, D.; Zhang, H.; Zou, X.; Bons, A. J. *Microporous Mesoporous Mater.* **2005**, *78*, 1.
(21) Choi, M.; Cho, H.; Srivastava, R.; Venkatesan, C.; Choi, D.; Ryoo, R. *Nat. Mater.* **2006**, *5*, 718.
(22) Mintova, S.; Olson, N.; Senker, J.; Bein, T. *Angew. Chem., Int. Ed.* **2002**, *41*, 2558.
(23) de Moor, P.; Beelen, T.; Van Santen, R. *J. Phys. Chem. B* **1999**, *103*, 1639.
(24) van Grieken, R.; Sotelo, J. L.; Menéndez, J. M.; Melero, J. A. *Microporous Mesoporous Mater.* **2000**, *39*, 135.
(25) Aguado, J.; Serrano, D. P.; Escola, J. M.; Rodríguez, J. M. *Microporous Mesoporous Mater.* **2004**, *75*, 41.
(26) Tsuji, K.; Jones, C. W.; Davis, M. E. *Microporous Mesoporous Mater.* **1999**, *29*, 339.
(27) Yamamoto, K.; Nohara, Y.; Domon, Y.; Takahashi, Y.; Sakata, Y.; Plévert, J.; Tatsumi, Y. *Chem. Mater.* **2005**, *17*, 3913.
(28) Serrano, D. P.; Aguado, J.; Escola, J. M.; Rodríguez, J. M.; Peral, A. *Chem. Mater.* **2006**, *18* (10), 2462.
(29) Serrano, D. P.; Aguado, J.; Escola, J. M.; Rodríguez, J. M.; Peral, A. *J. Mater. Chem.* **2008**, *18* (35), 4210.
(30) Aguado, J.; Serrano, D. P.; Rodríguez, J. M. *Microporous Mesoporous Mater.* **2008**, *115* (3), 504.
(31) Aguado, J.; Serrano, D. P.; Escola, J. M.; Peral, A. *J. Anal. Appl. Pyrol.* **2008**, DOI 10.1016/j.jaap.2008.10.009.

for 6 h. The organosilane was added in a proportion of 0−15 mol % with respect to the silica content in the gel. Finally, crystallization was carried out in Teflon lined stainless-steel autoclaves under static conditions and autogenous pressure at 170 °C for 7 days. The solid products obtained were separated by centrifugation, washed several times with distilled water, dried overnight at 110 °C, and calcined in air at 550 °C for 5 h.

Powder X-ray diffraction (XRD) patterns were measured using a Philips X'PERT MPD diffractometer (Cu Kα radiation) with step size and counting time of 0.02° and 10 s, respectively. Fourier transform infrared (FTIR) spectra were recorded in a Mattson Infinity Series spectrophotometer with a resolution of 4 cm^{-1} using the KBr pellet technique. The Si/Al atomic ratios of the catalysts were determined by inductively coupled plasma spectroscopy (ICP) with a VARIAN VISTA AX apparatus, while elemental chemical analyses for C, N, and H were carried out using a Vario EL III instrument. Thermogravimetric (TGA) and differential thermal (DTA) analyses were performed simultaneously using a SDT 2960 instrument. Transmission electron microscopy (TEM) images were obtained with a JEOL 2000 electron microscope operating at 200 kV.

Nitrogen adsorption−desorption isotherms at 77 K were obtained in a Micromeritics ASAP 2010 instrument, whereas argon adsorption−desorption isotherms at 87 K were acquired using a Quantachrome Autosorb 1 MP automated gas sorption system. In both cases, the analyses were carried out after outgassing the samples at 350 °C under vacuum for 16 h. BET surface analyses have been performed using the relative pressure range of 0.05−0.16 in the nitrogen adsorption isotherm as range of linearity (using a molecular cross-sectional area for N_2 of 0.162 nm^2). Argon adsorption isotherms were acquired at 87 K on selected samples and analyzed by applying nonlocal density functional theory (NLDFT). NLDFT describes the configuration of adsorbed molecules in pores on a molecular level and is considered to be the most accurate method for a comprehensive and accurate pore size analysis over a wide pore size range from 0.4−100 nm.[32−35] NLDFT kernels (methods) have been developed for many adsorptive/adsorbent systems and are meanwhile widely used in pore size analyses. (NLDFT is also featured in a new ISO standard that focuses on the analysis of micro- and mesopores by gas adsorption.[36]) The argon adsorption isotherms obtained on the ZSM-5 zeolites studied here were analyzed with a hybrid NLDFT method which assumes argon adsorption (at 87 K) in cylindrical siliceous zeolite pores in the nanopore range and an amorphous (cylindrical) silica pore model for the mesopore range.[34,35,37]

All solid-state ^1H, ^{13}C, ^{27}Al, and ^{29}Si NMR experiments were conducted at room temperature at a magnetic field strength of 11.7 T on a high-resolution Bruker AVANCE 500 NMR spectrometer operating at frequencies of 500 MHz for ^1H, 125.72 MHz for ^{13}C, 130.28 MHz for ^{27}Al, and 99.33 MHz for ^{29}Si. ^1H, ^{13}C, and ^{29}Si chemical shifts were referenced to the corresponding nuclei in tetramethylsilane, whereas ^{27}Al was referenced to a 1 M aqueous solution of $AlCl_3$. Magic-angle spinning (MAS) NMR spectra were obtained using a 4 mm Bruker double-resonance broadband MAS probehead with spinning rates of 12 kHz. Solid-state one-dimensional (1D) single-pulse ^1H MAS NMR spectra were recorded using a 1.7 μs $\pi/2$ pulse, a recycle delay of 300 s to allow complete relaxation of the ^{29}Si nuclei, and 32 transients. Solid-state 1D single-pulse ^{29}Si MAS NMR spectra were recorded using a 1.5 μs $\pi/2$ pulse, a recycle delay of 20 s, and 3000 transients. Solid-state 1D single-pulse ^{27}Al MAS NMR spectra were recorded with a 1.1 μs $\pi/4$ pulse, a recycle delay of 3 s, and 3000 transients. Solid-state 1D ^{29}Si CP-MAS NMR spectra were recorded with a ^1H $\pi/2$ pulse of 1.7 μs, followed by a 1 ms contact time for cross-polarization (CP), a recycle delay of 2 s, and 5000 transients. Solid-state 1D ^{13}C CP-MAS NMR spectra were recorded with a ^1H $\pi/2$ pulse of 1.7 μs, followed by a 2 ms CP contact time, a recycle delay of 2 s, and 3200 transients. Solid-state two-dimensional (2D) $^{29}Si\{^1H\}$ and $^{13}C\{^1H\}$ heteronuclear correlation (HETCOR) NMR experiments[38,39] were performed under MAS conditions at 12.0 kHz using a ^1H $\pi/2$ pulse of 1.7 μs, followed by a 3 ms CP contact time. High-power proton decoupling was applied during the detection periods to remove broadening effects from $^1H-^{29}Si$ or $^1H-^{13}C$ dipolar couplings. Time proportional phase incrementation (TPPI) was used for phase sensitivity.

Catalytic properties of the zeolite samples were tested for the cracking of low-density polyethylene (LDPE) with an average molecular weight of 416 000. The reactions were carried out in a stainless steel batch reactor provided with a helicoidal stirrer swept by a continuous nitrogen flow (35 $mL \cdot min^{-1}$) to ensure that the LDPE conversion takes place under inert conditions and to favor the removal of the volatile products. In a typical experiment, 10 g of LDPE were introduced into the reactor together with 0.1 g of the catalyst (LDPE/catalyst mass ratio of 100). The reactions were performed at 340 °C for 2 h.

3. Results and Discussion

The strategy applied here to obtain ultrasmall ZSM-5 nanocrystals is directly linked to the mechanism of zeolite crystallization from clear solutions. Although this mechanism is still the subject of controversy in the literature, significant progress has been recently achieved, providing insight on several crucial aspects.[40] In the case of zeolites with MFI topology, many authors have observed, in the earliest steps of the crystallization from clear solutions, the formation of nanoparticles with sizes in the range of 2−5 nm.[41−45] Characterization of these nanoparticles, such as by X-ray diffraction and NMR, has shown that while they appear to lack crystalline properties they contain significant amounts of the zeolite structure-directing agent (TPA^+ cations). Some authors have proposed that these nanoparticles are entities

(32) Neimark, A. V.; Ravikovitch, P. I. *Microporous Mesoporous Mater.* **2001**, *44*, 697.
(33) Thommes, M.; Smarsly, B.; Groenewolt, M.; Ravikovitch, P. I.; Neimark, A. V. *Langmuir* **2006**, *22*, 756.
(34) Ravikovitch, P. I.; Neimark, A. V. *Langmuir* **2006**, *22*, 10864.
(35) Thommes, M. *Stud. Surf. Sci. Catal.* **2007**, *168* (15), 495.
(36) ISO-15901-3: Pore size distribution and porosity of solid materials by mercury porosimetry and gas adsorption−Analysis of micropores by gas adsorption, 2007. ISO-15901−-2: Pore size distribution and porosity of solid materials by mercury porosimetry.
(37) (a) Ravikovitch, P. I.; Neimark, A. V. Personal Communication 2001. (b) Thommes, M. *Particle Technology News 4*; Quantachrome: Boynton Beach, FL 2001; Quantachrome Autosorb data reduction software version AS 1.52.
(38) Vega, A. J. *J. Am. Chem. Soc.* **1988**, *110*, 1049.
(39) Janicke, M. T.; Landry, C. C.; Christiansen, S. C.; Kumar, D.; Stucky, G. D.; Chmelka, B. F. *J. Am. Chem. Soc.* **1998**, *120*, 6940.
(40) Rimer, J. D.; Fedeyko, J. M.; Vlachos, D. G.; Lobo, R. F. *Chem. Eur. J.* **2006**, *12*, 2926.
(41) Persson, A. E.; Schoemann, B. J.; Sterte, J.; Otterstedt, J. E. *Zeolites* **1994**, *14*, 557.
(42) Schoeman, B. J.; Regev, O. *Zeolites* **1996**, *17*, 447.
(43) Nikolakis, V.; Kokkoli, E.; Tirrell, M.; Tsapatsis, M.; Vlachos, D. G. *Chem. Mater.* **2000**, *12*, 845.
(44) Jorge, M.; Auerbach, S. M.; Monson, P. A. *J. Am. Chem. Soc.* **2005**, *127*, 14388.
(45) Fyfe, C. A.; Darton, R. J.; Schneider, C.; Scheffler, F. *J. Phys. Chem. C.* **2008**, *112*, 80.

with well defined crystalline structures,[46] although others have suggested that their features are still far from those of the final zeolite.[45,47] Likewise, different alternatives have been proposed for the role(s) of these nanoparticles during zeolite crystallization. In several studies, they are proposed to act principally as a source of precursor species, assuming that they do not participate directly in the crystal growth, being dissolved as crystallization progresses.[48] Another possibility is that the nanoparticles are involved in or promote a mechanism of crystal growth by aggregation.[49] More recently, a mechanism has been proposed[50] reconciling several aspects among the different crystallization models by suggesting that the nanoparticles do not initially possess a well-ordered zeolite structure, although they evolve progressively into zeolite crystals through intermediate states involving growth by aggregation.

These achievements open opportunities for synthesizing zeolite nanocrystals with ultrasmall sizes by perturbing the crystallization process through organofunctionalization of the protozeolitic nanoparticles with a surface silanization agent (SSA). The main role of the silanization agent is to prevent aggregation of the nanoparticles into larger crystals during their evolution into particles with well-defined MFI structure. This novel strategy involves the following steps:

(i) Precrystallization of the zeolite synthesis gel to promote the formation of ZSM-5 precursor seed nanoparticles (nuclei). In addition to the silica and alumina sources, the gel includes tetrapropylammonium hydroxide (TPAOH), which is the most widely applied structure-directing agent (SDA) for producing the MFI zeolite topology. The duration and intensity of this step appear to be essential parameters, as they are expected to influence the nature and size of the first nuclei formed.

(ii) Functionalization of the zeolite seeds on their external surfaces by reaction with relatively bulky organosilanes. The organosilane species form a surface-passivating layer around the protozeolitic nanoparticles that prevents or significantly reduces their further aggregation. The most significant parameters in this step are related to the nature and amount of the surface-silanization agent (SSA) employed. In the present work, phenylaminopropyltrimethoxysilane (PHAPTMS) was used as the SSA species, based on its effectiveness in hindering the aggregation of zeolite nanocrystals, resulting in high-surface-area mesoporous zeolite products.[29]

(iii) Crystallization to complete the zeolitization of the functionalized seeds, as evidenced by high-angle X-ray diffraction reflections. If the silanization treatment has been effective in preventing crystal growth by aggregation, this step can be conducted at high hydrothermal temperatures, while maintaining the nanocrystalline features in the final product.

(46) Kirschhock, C. E. A.; Ravishankar, R.; Verspeurt, F.; Grobet, P. J.; Jacobs, P. A.; Martens, J. A. *J. Phys. Chem. B* **1999**, *103*, 4960.
(47) Kragten, D. D.; Fedeyko, J. M.; Sawant, K. R.; Rimer, J. D.; Vlachos, D. G.; Lobo, R. F.; Tsapatsis, M. *J. Phys. Chem. B* **2003**, *107*, 10006.
(48) Schoeman, B. J. *Microporous Mesoporous Mater.* **1998**, *22*, 9.
(49) Kirschhock, C. E. A.; Kremer, S. P. B.; Vermant, J.; Van Tendeloo, G.; Jacobs, P. A.; Martens, J. A. *Chem. Eur. J.* **2005**, *11*, 4306.
(50) Davis, T. M.; Drews, T. O.; Ramanan, H.; He, Ch.; Dong, J.; Schnablegger, H.; Katsoulakis, M. A.; Kokkoli, E.; McCormick, A. V.; Penn, R. L.; Tsapatsis, M. *Nat. Mater.* **2006**, *5*, 400.

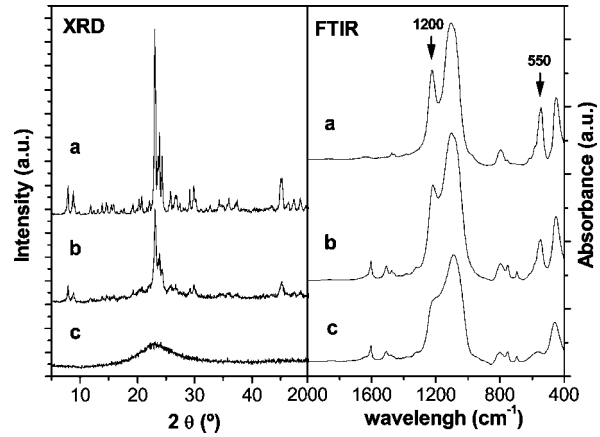

Figure 1. XRD patterns and FTIR spectra of as-synthesized zeolite materials prepared under different conditions: (a) 0% PHAPTMS with precrystallization at 90 °C, (b) with 12% PHAPTMS surface-silanization agent (SSA), and (c) without precrystallization at 90 °C.

(iv) Calcination at high temperature in air to remove the structure-directing and surface-silanization agents. Oxidation of the organic SDA and SSA species renders both the internal nanopores and external zeolite surfaces accessible for adsorption and catalysis.

Effect of Precrystallization. Whether a precrystallization treatment is necessary to form zeolite nuclei can be established by comparing syntheses with and without an induction period before the surface silanization agent is added. Accordingly, two otherwise identical samples were prepared under the same reaction conditions with 12 mol % of SSA, omitting for one of them the precrystallization step, so the silanization agent was added at the beginning of the gel preparation. For the second sample, a precrystallization step at 90 °C for 20 h was applied prior to the silanization treatment. Likewise, as a control, a third material was prepared without adding the silanization agent to the otherwise same gel, which was expected to lead to the formation of a conventional nanocrystalline ZSM-5 sample. Figure 1 shows the XRD patterns and FTIR spectra corresponding to these three materials. As expected, the material obtained without the SSA presents the X-ray pattern [Figure 1a, left] typical of ZSM-5 zeolite with well defined reflections. Likewise, its FTIR spectrum [Figure 1a, right] exhibits a band at 550 cm^{-1}, which is commonly assigned to pentasil units in the MFI zeolite topology, while the band at around 1200 cm^{-1} is clearly resolved, indicating the high crystallinity of this material. In the case of the sample obtained using both precrystallization and seed silanization, the same X-ray reflections are clearly identified [Figure 1b, left] but are less resolved with lower intensities, consistent with the presence of smaller crystallites under the influence of the silanization agent. The FTIR spectrum [Figure 1b, right] of the precrystallized and then seed-silanized product shows similar peaks that indicate its relatively high degree of framework ordering, albeit with somewhat broader linewidths than for conventionally crystallized ZSM-5. Finally, no reflections are detected in the X-ray pattern of the sample prepared without the precrystallization treatment [Figure 1c, left], which indicates that this material lacks long-range molecular order.

Furthermore, the FTIR spectrum of this sample [Figure 1c, right] corroborates its amorphous nature, with the 550 and 1200 cm^{-1} bands being observed only as low-intensity shoulders.

The above results provide important information about the crystallization mechanism and the role of the phenylaminopropyltrimethoxysilane silanization agent. When PHAPTMS is added at the earliest steps of the gel preparation, its presence strongly modifies the synthesis, inhibiting the growth of larger crystals of zeolite ZSM-5. In the absence of a precrystallization treatment, the silanization agent is mixed directly with the silica and aluminum sources (TEOS and IPA, respectively), each of which is collectively hydrolyzed and mutually co-condensed. Co-condensation reactions between hydrolyzed PHAPTMS and TEOS/IPA may lead to the formation of organofunctionalized aluminosilica oligomers that have nucleated, though not necessarily around zeolite-structure-directing TPA^+ cations. For such species, the presence of the large organic moieties associated with the silanization agent is expected to hinder their incorporation and crystallization into the MFI structure, which is consistent with the absence of crystallinity in the product obtained after hydrothermal treatment without a precrystallization step. By comparison, when the gel is subjected to precrystallization at 90 °C before the addition of the silanization agent, crystalline MFI zeolite is obtained, though with particle sizes depending on the duration of the precrystallization time. This suggests that protozeolitic nanoparticles form during the precrystallization treatment, as structure-directing TPA^+ cations co-assemble with anionic aluminosilica species. This is consistent with a previous work,[28] where thermogravimetric analyses of the X-ray amorphous material obtained after the precrystallization treatment revealed the presence of TPA^+ species strongly retained in the solid product. These results confirm the importance of the precrystallization step to promote the formation of protozeolitic seeds prior to the addition of the silanization agent. However, as indicated above, the material at the end of the precrystallization stage is still X-ray amorphous. Hence stronger crystallization conditions (longer times and/or higher temperatures) must be employed to increase the extent of zeolite crystallization.

Effect of Precrystallization Temperature and SSA Concentration. A number of factors are essential for the formation of ZSM-5 nanocrystals (<10 nm) from silanized seeds, including the temperature and duration of the precrystallization step and the type and concentration of the silanization agent. PHATPMS is an effective surface-silanization agent, due to its hydrophilicity and relatively large molecular size. Two series of nanocrystalline zeolite samples (denoted as "*n*-ZSM-5") were prepared at low and high precrystallization temperatures, 40 °C (LTP-*x*) and 90 °C (HTP-*x*), respectively, and by varying the concentration of PHAPTMS silanization agent used at a fixed precrystallization time of 20 h. For both series, the amount of the silanization agent added after the precrystallization step was varied from $x = 0$ to $x = 15$ mol %, relative to the total silica content of the gel. All other synthesis compositions and conditions were kept constant, as described in the Experimental Section.

Figure 2 shows representative TEM images of several ZSM-5 zeolite products prepared from silanized seeds, as compared with the conventionally crystallized ZSM-5 reference material obtained by omitting the silanization step under otherwise identical conditions. As shown in Figure 2a,b, the latter is formed by aggregates of nanocrystals with sizes in the range 40−70 nm and can be considered as a "standard" nanocrystalline ZSM-5 zeolite. By comparison, the morphologies of the ZSM-5 products prepared from silanized seeds shown in Figure 2(c−f) are significantly different. They consist of relatively large 300-nm sponge-like aggregates of much smaller nanoparticles. This relatively large size of the aggregates is a positive fact as it favors the recovery of the synthesis product by centrifugation, which otherwise would be very difficult if the nanocrystals were completely isolated. Small individual nanoparticles appear to be crystalline, as evidenced by both electron diffraction measurements and the lattice fringes observed in the high resolution TEM images. These crystalline features are evident, despite the extremely small size of the individual zeolite nanoparticles. Note that in many cases the nanocrystal sizes are well below 10 nm, with an average size around 5 nm, which is one of the smallest values thus far reported for ZSM-5 zeolite.

Interestingly, in several regions of the images [Figure 2d,f], the lattice fringes exhibit the same orientations in regions extending over several nanocrystallites. Therefore, the effective size of the crystalline domains seems to be somewhat larger than that of the individual nanocrystals, suggesting that the nanoparticles are not completely independent and that partial intergrowth has occurred through and developed across nanocrystal contact points. It is furthermore noteworthy that the sizes of the individual nanocrystals prepared here by surface silanization are similar to those of the nanoparticles (2−5 nm) identified by a number of authors in the early stages of the crystallization of MFI zeolites from clear solutions.[41−44] This suggests that there may be a direct relationship between the two. Moreover, the sponge-like aspect of the large particles indicates that crystal growth can take place by an aggregative mechanism of smaller nanoparticle nucleates, whereas in the absence of the SSA under hydrothermal conditions, prezeolite nanoparticles can nucleate, aggregate, merge, and grow into larger and more compact crystals;[50] grafting of the organosilanization agent onto the protozeolitic precursors passivates their exterior particle surfaces and inhibits the extents of their aggregation and merged growth. The passivated protozeolitic precursors continue to crystallize during the final hydrothermal treatment on a time scale similar to conventional ZSM-5 syntheses though maintain their ultrasmall dimensions with little aggregative growth or fusion.

All of the samples, prepared under both low- and high-temperature precrystallization conditions, present XRD patterns [see Supporting Information] that are typical of the MFI structure, establishing that even a mild precrystallization at 40 °C is sufficient to induce the formation of zeolite precursors that, after the silanization treatment, can be converted into zeolite nanocrystals. The materials obtained from silanized seeds exhibit reflections of lower intensity compared to the reference ZSM-5 sample prepared in the

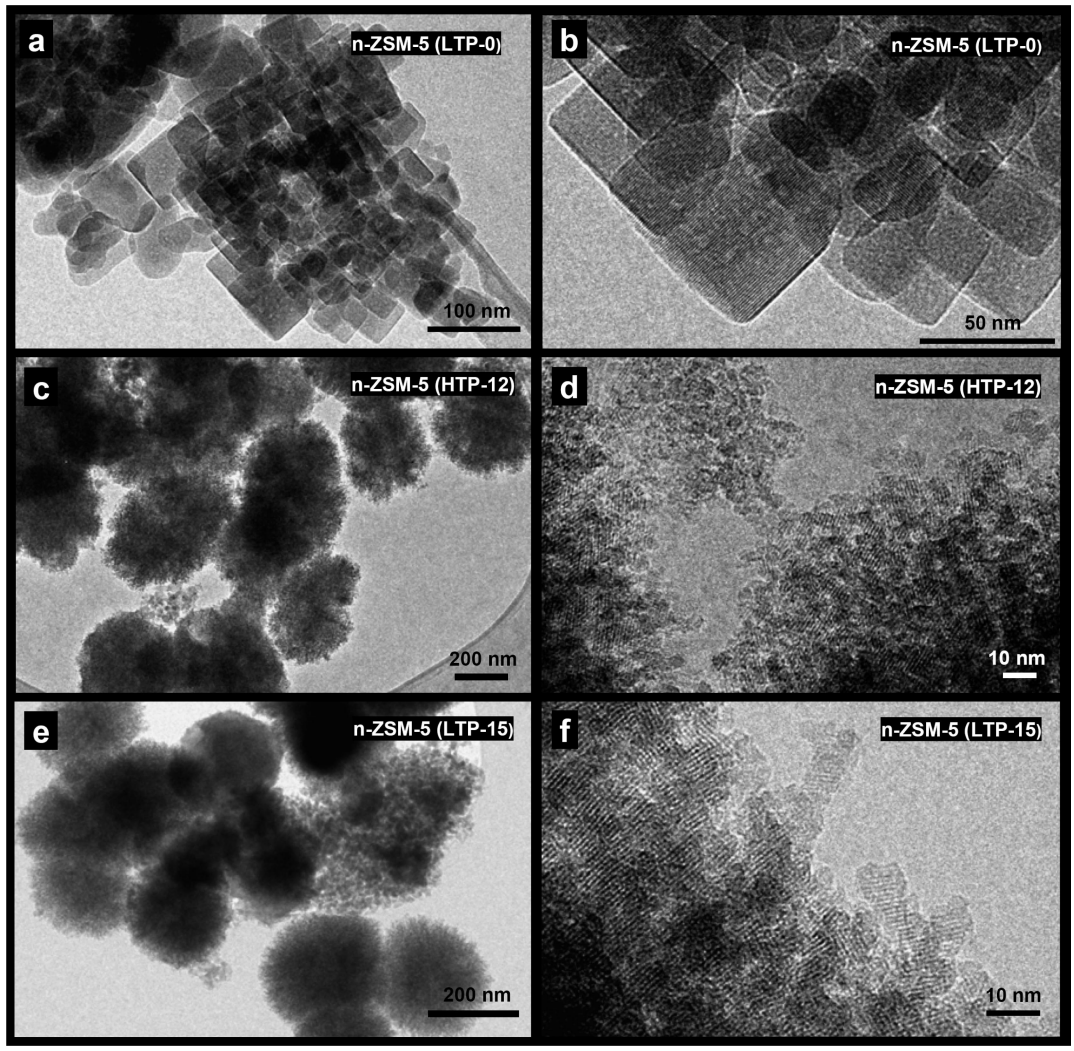

Figure 2. Representative TEM micrographs of calcined nanocrystalline *n*-ZSM-5 zeolites prepared with (a, b) 0% PHAPTMS and precrystallized at 40 °C, (c, d) 12% PHAPTMS and precrystallized at 90 °C, and (e, f) 15% PHAPTMS and precrystallized at 40 °C.

absence of PHATPMS, suggesting a reduction in the mean crystallite sizes. This effect is more pronounced for the samples precrystallized at 40 °C (LTP series), which is consistent with milder precrystallization temperatures leading to the formation of smaller protozeolitic nanoparticles in the synthesis gel.

FTIR spectra [see also Supporting Information] of the as-synthesized products of low- and high-temperature precrystallization and subsequent silanization treatments show vibrational bands that are characteristic of crystalline zeolites. The band at about 550 cm^{-1} is clearly present in all of the samples, which confirms the high degree of local framework ordering in these materials, consistent with their "nanocrystal" designation. The ratio of the intensities of the FTIR bands at 550 and 450 cm^{-1} has been proposed as an approximate measurement of the degree of crystallinity in MFI zeolites. However, this parameter is expected to depend on crystal size when approaching nanoscale dimensions, due to the influence of the external surface, associated defects, and discontinuity of the ordered framework structure for zeolite crystals with very small sizes. These external surfaces are expected to be terminated mainly by silanol groups, which inherently disrupt the pentasil units. The intensity ratios of the 550 and 450 cm^{-1} vibrational bands decrease across each series, as the amount of PHATPMS is increased, from 0.86 for the crystalline reference ZSM-5 product to approximately 0.7 for the materials prepared with the highest concentration of surface silanization agent. These changes correlate well with a reduction of the mean nanocrystallite sizes of the ZSM-5 zeolite products and the associated decrease in the number of intact pentasil units, as the influence of the external nanocrystallite surfaces becomes more important.

Surface silanization of the protozeolitic precursor nanoparticles has important impacts on the porosity and therefore textural properties of the materials.[29] This is evident in the N_2 adsorption−desorption isotherms for the products obtained from low- and high-temperature precrystallization treatments with different mole percents of the PHAPTMS surface silanization species [see Supporting Information]. The analysis of the adsorbed amount of N_2 at both low and intermediate relative pressures demonstrates that the ZSM-5 zeolites prepared from silanized seeds possess significantly higher porosities than the ZSM-5 reference material. This effect is strongly correlated with the concentration of silanization agent introduced during the syntheses. For both the low- and high-temperature precrystallization series, maximum N_2 adsorption occurs for ZSM-5 prepared from seeds silanized with 12 mol % of PHAPTMS, further

Table 1. Properties of ZSM-5 Materials Following Different Precrystallization and Hydrothermal Synthesis Treatments

sample	SSA (gel) (mol %)	SSA (solid) (mol %)	SDA (solid) (wt %)	Si/Al (solid)	S_{BET} (m^2/g)	yield[a] (%)
		LTP Series (precrystallization at 40 °C for 20 h)				
n-ZSM-5 (LTP-0)	0	0	12.2	29	419	78
n-ZSM-5 (LTP-5)	5	4.3	12.1	31	576	84
n-ZSM-5 (LTP-8)	8	6.1	11.2	32	610	81
n-ZSM-5 (LTP-12)	12	11.4	9.9	33	785	87
n-ZSM-5 (LTP-15)	15	13.5	10.7	34	705	86
		HTP Series (precrystallization at 90 °C for 20 h)				
n-ZSM-5 (HTP-0)	0	0	12.2	30	434	80
n-ZSM-5 (HTP-5)	5	5.1	11.0	34	545	93
n-ZSM-5 (HTP-8)	8	5.6	13.4	34	555	100
n-ZSM-5 (HTP-12)	12	10.4	11.8	36	698	100
n-ZSM-5 (HTP-15)	15	13.8	10.3	36	579	100

[a] Synthesis yield referred to starting gel compositions: $g_{calcinedsample}/(g_{SiO2} + g_{Al2O3})_{synthesis}$.

increasing in the concentration of the SSA to 15 mol % yielding diminished N_2 adsorption. This fact points to less beneficial influences on the macroscopic properties resulting from zeolite seed silanization treatments at high SSA concentrations. This may be due to increased viscosities of the synthesis gels when higher concentrations of PHAPTMS are present, which could hinder interactions and grafting of the organosilane species with the protozeolitic particles or increased possibility of homocondensation reactions between PHAPTMS molecules.

The BET surface areas of the different samples, calculated from the N_2 adsorption isotherms, are shown in Table 1. Although the BET equation is known not to be strictly valid for microporous solids, it is often used as a standard method that allows the surface areas of different samples to be estimated and compared.[51] The crystalline reference ZSM-5 samples were determined to have BET surface areas of 419 and 434 m^2/g for the low- and high-temperature precrystallization treatments, respectively. These values agree well with that typical for standard MFI zeolites,[52] approximately 400 m^2/g. In contrast, the samples prepared from silanized seeds show significantly higher BET surface areas, approaching 800 m^2/g, which increase with the concentration of surface-silanization agent to 12 mol % of PHAPTMS for precrystallization at either 40 or 90 °C. Increases of the BET surface area have been observed previously for nanocrystalline zeolites obtained by different methods and attributed to less restrictive N_2 adsorption on the relatively large external surface areas of small zeolite crystals, compared to adsorption within the zeolite nanopores.[25] The BET surface areas for ZSM-5 products prepared from silanized seeds appear to yield maxima of 785 and 698 m^2/g for 12 mol % of PHAPTMS for the low- and high-temperature precrystallization treatments, respectively. These figures denote a very important improvement of the textural properties regarding previous works on the ZSM-5 synthesis from silanized seeds, indicating that the variables here studied (precrystallization temperature and PHAPTMS amount) are very effective for enhancing and controlling the features of hierarchical ZSM-5. The significantly higher surface areas measured for products precrystallized at 40 °C, compared to 90 °C, confirm that a more effective surface functionalization is achieved at the lower temperature. Moreover, to the best of our knowledge, the value of 785 m^2/g is the highest BET surface area thus far reported for nanocrystalline ZSM-5 zeolites, consistent with the extremely small size of the nanocrystals prepared from silanized seeds. Interestingly, this BET surface area is also very close to the upper values reported for delaminated zeolites.[53] It is also noteworthy that the BET surface areas measured for the mesoporous ZSM-5 zeolites synthesized by the method described here are higher than those reported for similar materials with prepared by using amphiphilic organosilanes.[54,55] This is likely due to the smaller sizes of the protozeolitic nanocrystals formed at the initial stages of the current synthesis protocol.

Hierarchical Porosity. As discussed above, ZSM-5 products of silanized seed syntheses tend to be comprised of nanocrystal aggregates that result in complicated particle assemblies, morphologies, and associated porosities. The distributions of pore dimensions in ZSM-5 prepared from silanized seeds versus conventional syntheses can nevertheless be quantified and compared by using nonlocal density functional theory to analyze Ar adsorption isotherm data. Resulting analyses in Figure 3a,b yield cumulative pore volume and pore size distributions for calcined nanocrystalline ZSM-5 zeolite materials prepared under high-temperature precrystallization (90 °C) conditions without and with (12 mol %) PHAPTMS surface-silanization species. Both the conventional and the seed-silanized ZSM-5 products yield prominent peaks in their respective pore-size distributions at approximately 0.52 nm, a value that agrees very well with the dimension of the MFI nanopores. By comparison, for the ZSM-5 material obtained from silanized seeds, the main peak in the distribution centered at 0.52 nm is less intense than for the reference ZSM-5 sample, and a new and broader peak is observed in the mesopore range 2.0−4.0 nm. This result establishes the presence of additional porosity, which arises as a result of the interstitial voids existing between the nanocrystals, as observed in the TEM images (Figure 2). Moreover, the values included in Figure 3 show that the mesopore volume (V_{MES}) of the *n*-ZSM-5 (HTP-12) material, determined for pore sizes ranging from 1.6 to 50 nm, is approximately 0.51 cm^3/g, which is significantly higher than the corresponding mesopore volume associated with the zeolitic nanopores in this sample (around 0.25 cm^3/g). The same trend

(51) Walton, K. S.; Snurr, R. Q. *J. Am. Chem. Soc.* **2007**, *129* (27), 8552.
(52) Kokotailo, G. T.; Lawton, S. L.; Olson, D. H.; Meier, W. M. *Nature* **1978**, *272*, 437.
(53) Corma, A.; Fornés, V.; Rey, F. *Adv. Mater.* **2002**, *14* (1), 71.
(54) Srivastava, R.; Choi, M.; Ryoo, R. *Chem. Commun.* **2006**, 4489.
(55) Shetti, V. N.; Kim, J.; Srivastava, R.; Choi, M.; Ryoo, R. *J. Catal.* **2008**, *254*, 296.

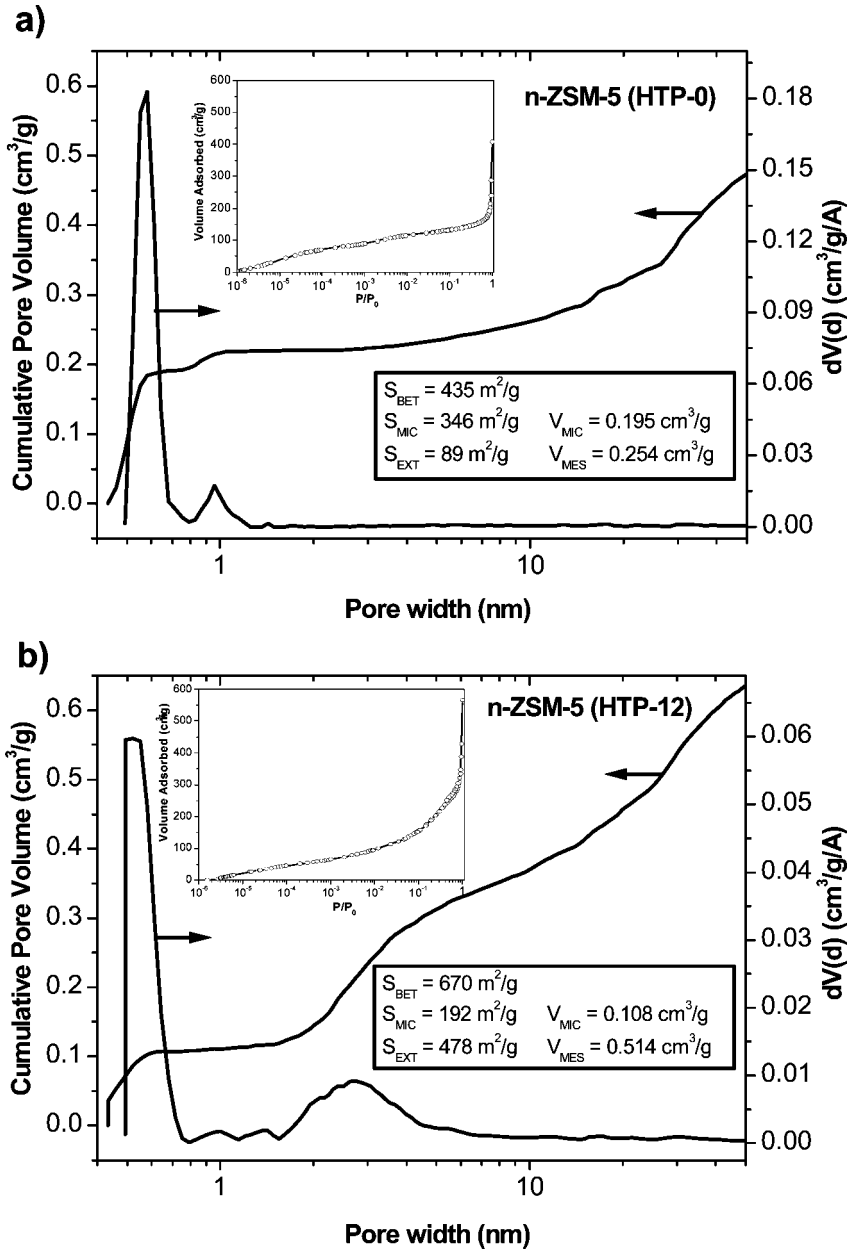

Figure 3. Cumulative pore volume and pore size distributions for calcined nanocrystalline *n*-ZSM-5 materials prepared under high-temperature precrystallization (HTP, 90 °C) conditions with (a) 0% and (b) 12% PHAPTMS surface-silanization agent. The distributions were obtained from NLDFT calculations applying a cylindrical pore model and using the adsorption branch of Ar adsorption−desorption isotherms (insets) at 87 K plotted on logarithmic scales. Nomenclature: BET surface area (S_{BET}); micropore surface area (S_{MIC}); external surface area (S_{EXT}) estimated as the difference $S_{BET} - S_{MIC}$; micropore volume (V_{MIC}) determined for pore sizes below 1.6 nm; and mesopore volume (V_{MES}) determined for pore sizes ranging from 1.6 to 50 nm.

is observed for the external surface (S_{EXT}) parameter, estimated as the difference between the total BET surface area and the micropore surface area (478 m^2/g for the sample with 12% of PHAPTMS vs 89 m^2/g for the material prepared in absence of surface-silanization agent). The ZSM-5 material obtained from silanized seeds, thus, exhibits an interesting hierarchical pore structure, which is expected to increase the relative importance of active sites on the external nanocrystal surfaces and to increase reactant accessibility to active sites within the intrananoparticle nanopores. The mesoporous surface area and the resulting enhanced accessibility to the internal acid sites are expected to make these materials promising catalysts for reactions otherwise hindered by steric and/or diffusional limitations.

Crystallization Yield and Al Incorporation. A usual drawback of the methods reported in the literature for syntheses of nanocrystalline zeolites is the low crystallization yields that are often obtained.[56] By comparison, as shown in Table 1, syntheses of ZSM-5 from silanized seeds proceed with very high yields, reaching values well over 90%. This is an important improvement in the crystallization of zeolite ZSM-5 with ultrasmall crystal sizes, compared to synthesis yields under low temperature crystallizations, which have been reported to be in the range of 20−25%.[25] In the approach described here, the silanized seeds were hydrothermally treated at high temperature (170 °C) under autog-

(56) Cundy, C. S.; Forrest, J. O.; Plaisted, R. J. *Microporous Mesoporous Mater.* **2003**, *66*, 143.

enous pressure. These relatively intensive crystallization conditions allow high synthesis yields to be achieved, while the presence of the silanization agent grafted onto the exterior surfaces of the zeolitic seeds prevents their aggregation and growth into large crystals.

Most of the catalytic applications of ZSM-5 zeolites require the presence of Al heteroatoms in the aluminosilicate lattice to generate framework acid sites. As shown in Table 1, the Si/Al ratios of the different as-synthesized samples are very similar to those present in the corresponding starting mixtures after seed silanization (Si/Al = 30−35, depending on the amount of SSA employed). This result indicates that Si and Al species are co-condensed into the zeolite framework without the silanization agent, noticeably affecting the extent to which the Al heteroatoms are incorporated. This is likely because the Al atoms are incorporated stably into the zeolitic seeds during the precrystallization step. Moreover, no significant variations are observed in the extent of Al incorporation into the different nanocrystalline ZSM-5 products prepared under low- and high-temperature precrystallization conditions, showing that even mild precrystallization at 40 °C is sufficient to promote the formation of aluminum-containing seeds.

The state and coordination of the Al species in the as-synthesized ZSM-5 products have been investigated by solid-state ^{27}Al MAS NMR spectroscopy [see Supporting Information]. The ^{27}Al MAS NMR spectra show a single signal centered at approximately 54 ppm that is assigned to four-coordinated Al atoms in aluminosilicate lattices, consistent with the incorporation of Al species into the ZSM-5 zeolite framework. The ^{27}Al linewidths associated with the peak at 54 ppm are slightly larger (∼6−7 ppm, full-width-at-half-maximum, fwhm) for the nanocrystalline ZSM-5 materials prepared from silanized seeds, compared to the crystalline ZSM-5 reference sample (5.8 ppm, fwhm). Nevertheless, they are still significantly narrower than ^{27}Al signals that are typically associated with amorphous silica−alumina materials (∼12−15 ppm, fwhm).[57] Consequently, the high fractions of exterior particle surface sites in the nanocrystalline ZSM-5 materials appear to contribute modestly to more heterogeneous distributions of local Al environments, while retaining principally crystalline features.

SSA Location and Distribution. The results above indicate clearly that the incorporation of PHAPTMS surface silanization species during synthesis can have a strong influence on ZSM-5 zeolite properties by altering the extent to which crystal growth can occur. To establish how the PHAPTMS or other silanization agents induce these changes, the compositions and structures of the nanocrystalline ZSM-5 materials were examined in bulk by elemental analyses and at a molecular level by one- (1D) and two-dimensional (2D) solid-state NMR spectroscopy. Bulk elemental analyses yield the mole percents of both the TPA^+ zeolite structure-directing agent (SDA) and PHAPTMS surface-silanization agent (SSA) in the different ZSM-5 products, as functions of their concentrations in the initial synthesis gels and the precrystallization temperature. As shown in Table 1, while the TPA^+ contents of the products undergo modest systematic variations across each precrystallization series, the proportion of SSA in each of the final ZSM-5 products tracks closely that in the initial synthesis gel, indicating that the PHAPTMS efficiently grafts to the zeolitic seeds.

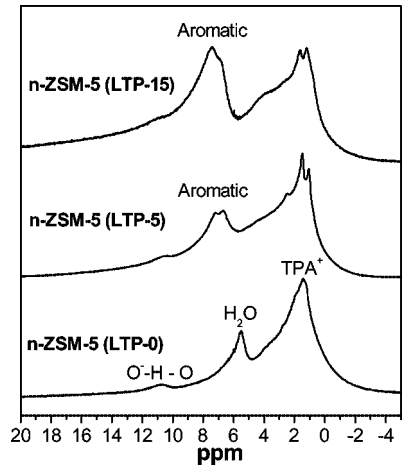

Figure 4. Solid-state ^{1}H MAS NMR spectra acquired at room temperature of as-synthesized nanocrystalline *n*-ZSM-5 zeolites prepared under low-temperature precrystallization (LTP, 40 °C) conditions with different SSA contents: (bottom) 0% PHAPTMS (LTP-0), (middle) 5% PHAPTMS (LTP-5), and (top) 15% PHAPTMS (LTP-15).

More detailed molecular insights on the proximities of the PHAPTMS surface-silanization agent and structure-directing TPA^+ species are provided by solid-state 1D and 2D NMR techniques. For example, ^{1}H MAS NMR spectra are shown in Figure 4 for three ZSM-5 products prepared using a precrystallization temperature of 40 °C and different concentrations (0, 5, and 15 mol %) of the surface-silanizing PHAPTMS species. In the absence of any silanization agent [Figure 4 (bottom)], the most intense ^{1}H resonance at about 1.5 ppm corresponds to the alkyl protons in TPA^+ molecules, whereas secondary resonances are attributed to water molecules (at 5.5 ppm) and hydrogen-bonded protons (at 11 ppm).[58] By comparison, nanocrystalline ZSM-5 materials prepared from silanized seeds precrystallized at 40 °C present a number of additional strong signals in the range 6−8 ppm [Figure 4 (middle, top)], arising from the presence of aromatic protons, and at 1.0 and 1.8 ppm for the propyl proton moieties in the PHAPTMS molecules. These ^{1}H signals become more intense with increasing contents of the PHAPTMS silanization species at 5 mol % and 15 mol %.

Solid-state ^{13}C cross-polarization magic-angle-spinning (CP-MAS) NMR spectra yield greater resolution of signals from the organic zeolite structure-directing and surface-silanizing species. Figure 5 shows ^{13}C CP-MAS NMR spectra for the same as-synthesized ZSM-5 materials examined in Figure 4. For the crystalline ZSM-5 reference material [Figure 5 (bottom)], different ^{13}C signals at 10.0 and 11.0 ppm, 16 ppm, and 63 ppm are resolved from distinct carbon moieties associated with the TPA^+ propyl chains. The signals at 10.0 and 11.0 ppm have been attributed to TPA^+ methyl groups in different nonsymmetric arrangements in the linear

(57) Oldfield, E.; Haase, J.; Schmitt, K. D.; Schramm, S. E. *Zeolites* **1994**, *14*, 101.

(58) Parker Jr., W. O.; Millini, R. *J. Am. Chem. Soc.* **2006**, *128*, 1450.

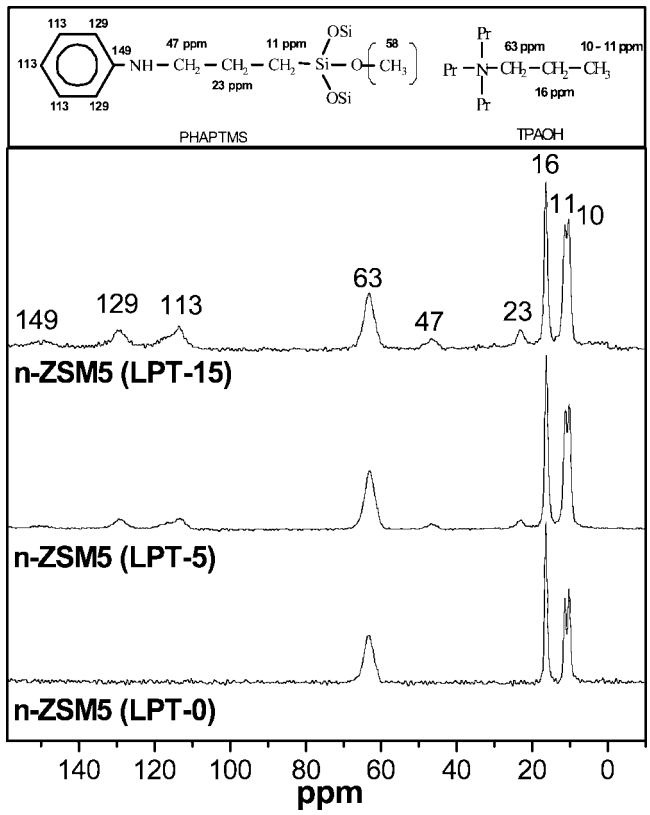

Figure 5. Solid-state ^{13}C CP-MAS NMR spectra acquired at room temperature of the same as-synthesized nanocrystalline *n*-ZSM-5 zeolites as measured in Figure 4, prepared under low-temperature precrystallization (LTP, 40 °C) conditions with different SSA contents: (bottom) 0% PHAPTMS (LTP-0), (middle) 5% PHAPTMS (LTP-5), and (top) 15% PHAPTMS (LTP-15). The molecular structures of the PHAPTMS surface-silanization and TPAOH zeolite structure-directing agents are shown at the top, along with the isotropic ^{13}C chemical shifts of the different carbon moieties in the compounds.

and sinusoidal channels of the MFI structure.[59,60] These signals are also present in the ^{13}C CP-MAS spectra of the nanocrystalline ZSM-5 materials prepared from silanized seeds [Figure 5(middle, top)], along with ^{13}C signals at 23, 47, 113, 129, and 149 ppm from the PHAPTMS species. The lower and broader relative signal intensities associated with PHAPTMS species, compared to TPA^+, are consistent with their less ordered environments on the exterior ZSM-5 nanocrystal surfaces, which contribute significantly to the overall surface area.

Solid-state single-pulse ^{29}Si MAS NMR spectra [see Supporting Information] of these same samples provide complementary quantitative information on type and relative populations of framework and silanized ^{29}Si species. Partially resolved ^{29}Si resonances were observed in the region −100 to −105 ppm corresponding to different Q^3(0 Al) and Q^4(1 Al) ^{29}Si sites and at approximately −110 to −115 ppm associated with Q^4(0 Al) ^{29}Si sites in the crystalline ZSM-5 reference product.[61] Notably, for the nanocrystalline ZSM-5 materials, a broad ^{29}Si resonance is also clearly observed at approximately −68 ppm, corresponding to T^3, $RSi(OSi)_3$, organosiloxane moieties that originate from the PHAPTMS silanization species. Comparing the integrated intensities of the ^{29}Si signals indicates that the relative fraction of silicon atoms corresponding to T^3 organosiloxane species (4.8 and 16.2 mol %, respectively) is close to the theoretically expected value for the content of PHAPTMS in the synthesis gels (5 and 15 mol %, respectively). However, while the ^{29}Si signal from the T^3 moieties confirms the presence of organosiloxane moieties in the bulk samples, it does not establish directly whether or to what extent they are associated to the nanocrystalline ZSM-5 frameworks or surfaces.

Detailed and unambiguous information on the interactions, locations, and distributions of the structure-directing and surface-silanization species is provided by high-resolution 2D NMR spectroscopy, which correlates signals from molecularly proximate species. Specifically, 2D $^{13}C\{^1H\}$ and $^{29}Si\{^1H\}$ heteronuclear chemical-shift correlation spectroscopy (HETCOR) NMR can correlate and distinguish signals from various ^{13}C or ^{29}Si moieties that are dipole−dipole coupled to protons associated with the phenylaminopropyltrimethoxysilane surface-silanization species and with the ZSM-5 structure-directing tetrapropylammonium cations in as-synthesized ZSM-5 materials. Figure 6 depicts solid-state $^{13}C\{^1H\}$ HETCOR NMR spectra for conventionally crystallized reference ZSM-5 and nanocrystalline ZSM-5 prepared from silanized seeds (precrystallization at 40 °C and 15 mol % PHAPTMS). For sufficiently short mixing times (here, 3 ms), only correlations between near-neighbor atomic species are observed. The reference ZSM-5 material corresponds to the same sample as examined in Figures 2(a,b), 4 (bottom), and 5 (bottom), while the nanocrystalline ZSM-5 material is the same as examined in Figures 2(e,f), 4 (top), and 5 (top). Separately acquired solid-state 1D ^{13}C CP-MAS and single-pulse ^1H MAS spectra are plotted along their respective axes to facilitate the interpretation of the 2D HETCOR spectra. In the 2D $^{13}C\{^1H\}$ HETCOR spectrum shown in Figure 6a for the crystalline ZSM-5 reference, strong correlated 2D signal intensities are observed at 1.5 ppm in the ^1H dimension and at 10, 11, 16, and 63 ppm in the ^{13}C dimension from the propyl moieties associated with the TPA^+ cations. Less intense ^1H signals attributed to adsorbed water (5.5 ppm) and H-bonded (10.5 ppm) protons yield no or very weak ^{13}C intensity correlations, indicating that they do not interact strongly with the TPA^+ carbon moieties. In Figure 6b for the nanocrystalline ZSM-5 product, these same correlations are present, with an additional intensity contributed by the propyl linking groups associated with the PHAPTMS. More importantly, strong correlated signals are also observed at 6−8 ppm in the ^1H dimension and at 113, 129, and 149 ppm in the ^{13}C dimension, corresponding to aromatic moieties of the PHAPTMS surface-silanization species. Consequently, based on the 2D $^{13}C\{^1H\}$ HETCOR spectra in Figure 6, the strong ^1H signals at 6−8 ppm are unambiguously assigned to silanizing PHAPTMS species, whereas the strong though broad ^1H signals in the range 1−2 ppm are mainly attributed to the structure-directing TPA^+ (with a smaller contribution from the propyl proton moieties in the PHAPTMS molecules).

(59) Nagy, J. B.; Gabelica, Z.; Derouane, E. G. *Zeolites* **1983**, *3*, 43.
(60) Kovalakova, M.; Wouters, B. H.; Grobet, P. J. *Microporous Mesoporous Mater.* **1998**, *22*, 193.
(61) Martínez-Morales, E.; Fripiat, J. J.; Alvarez, L. J. *Chem. Phys. Lett.* **2001**, *349*, 286.

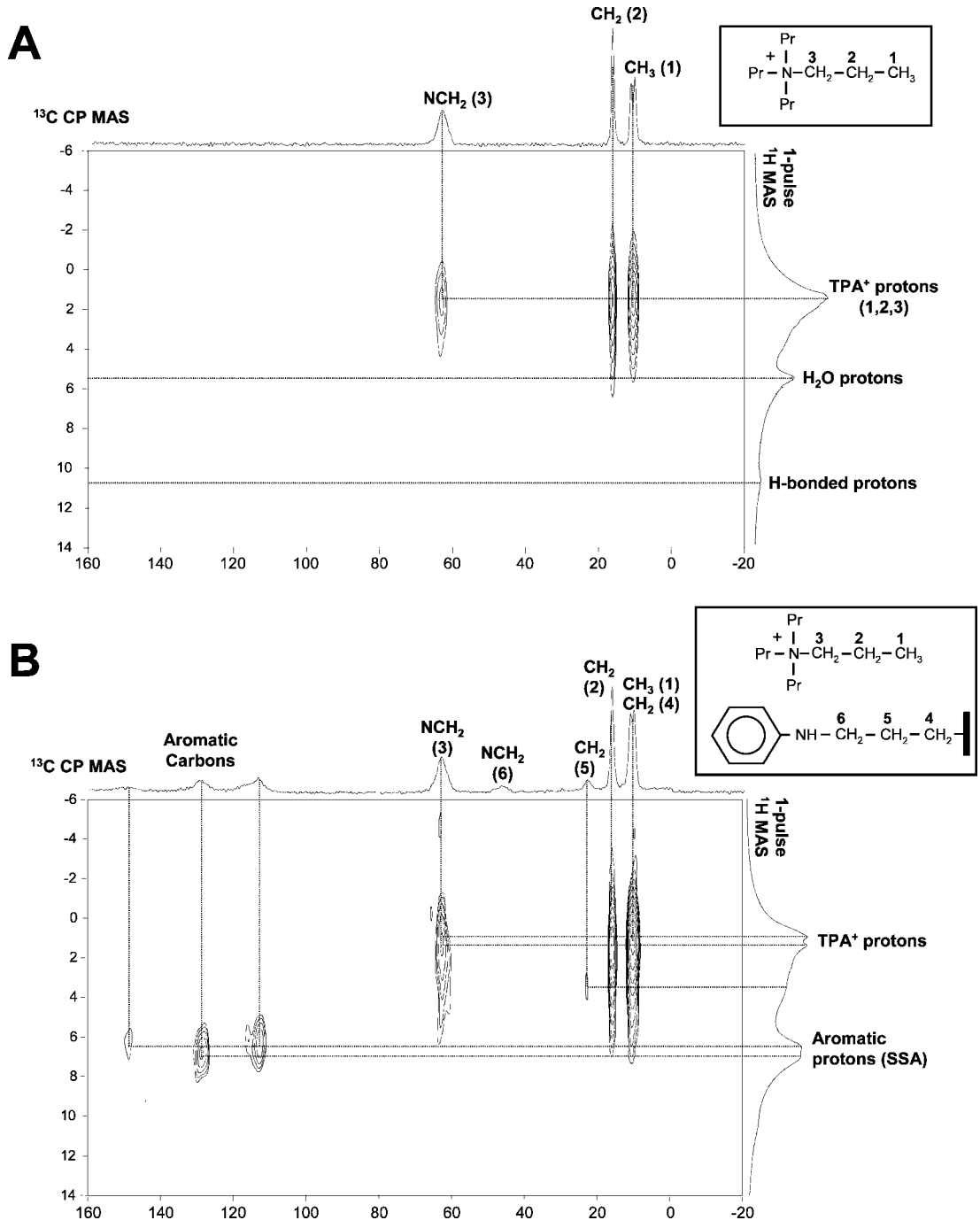

Figure 6. Solid-state 2D ^{13}C{^{1}H} HETCOR NMR spectra acquired at room temperature of the same as-synthesized nanocrystalline *n*-ZSM-5 zeolites as measured in Figures 4a,c and 5a,c, prepared under low-temperature precrystallization (LTP, 40 °C) conditions with (A) 0% PHAPTMS (LTP-0) and (B) 15% PHAPTMS (LTP-15). Separate ^{13}C CP-MAS NMR and single-pulse ^{1}H MAS NMR spectra are plotted along their respective axes to facilitate assignments of the intensity correlations observed. Short 3-ms CP contact times were used to probe molecularly proximate species. The alkyl ^{13}C signals are labeled according to the numerical designations of the different carbon moieties in the accompanying molecular structures of PHAPTMS and TPAOH.

With the assignment of ^{1}H NMR signals to the distinct zeolite structure-directing and surface-silanization species, their locations and distributions with respect to the zeolite nanocrystals can be established by using 2D ^{29}Si{^{1}H} HETCOR NMR. Figure 7 shows solid-state 2D ^{29}Si{^{1}H} HETCOR spectra on the same as-synthesized ZSM-5 samples as described in Figure 6. In Figure 7a for the crystalline ZSM-5 reference, strong correlated 2D signal intensities are observed at 1.5 ppm in the ^{1}H dimension and at −105 and −110 ppm in the ^{29}Si dimension, establishing unambiguously strong molecular associations between the propyl moieties of the TPA$^+$ cations and Q^4 and Q^3 silicate sites in the crystalline ZSM-5 framework. A weak intensity correlation is also observed at 10.5 ppm in the ^{1}H dimension and at −103 ppm in the ^{29}Si dimension, which is attributed to H-bonded protons interacting with Q^3 ^{29}Si sites, most likely silanol defects. Similarly, these same intensity correlations are observed in the 2D ^{29}Si{^{1}H} HETCOR spectrum in Figure 7b for the nanocrystalline ZSM-5 product prepared in the presence of PHAPTMS following precrystallization at 40 °C. In addition, correlated (albeit weaker) signal intensity is also observed at 1.5 ppm and 7.0 in the ^{1}H

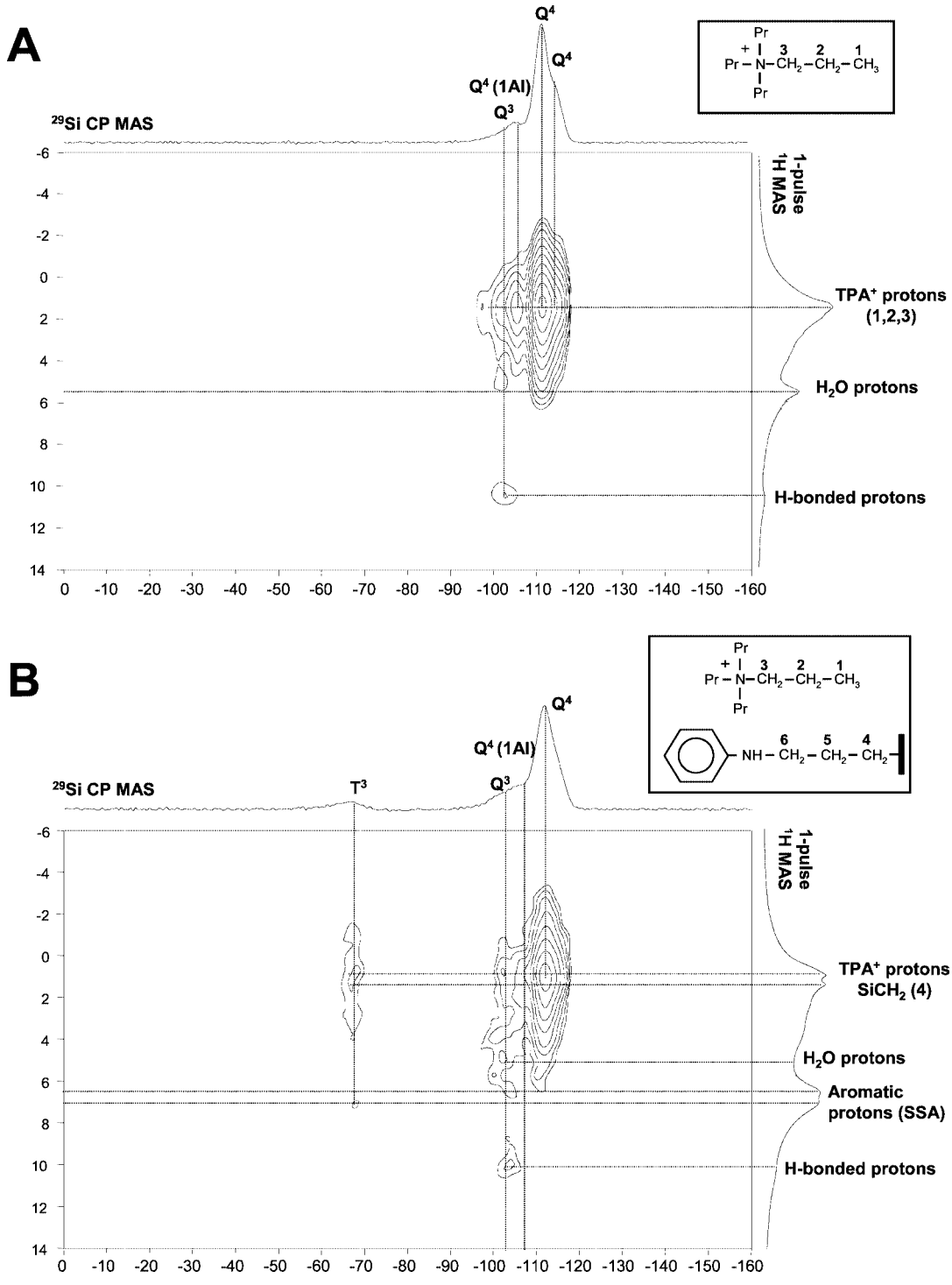

Figure 7. Solid-state 2D $^{29}Si\{^{1}H\}$ HETCOR NMR spectra acquired at room temperature of the same as-synthesized nanocrystalline *n*-ZSM-5 zeolites as measured in Figures 4a,c, 5a,c, and 6 prepared under low-temperature precrystallization (LTP, 40 °C) conditions with (A) 0% PHAPTMS (LTP-0) and (B) 15% PHAPTMS (LTP-15). Separate ^{29}Si CP-MAS NMR and single-pulse ^{1}H MAS NMR spectra are plotted along their respective axes to facilitate assignments of the intensity correlations observed. Short 3-ms CP contact times were used to probe molecularly proximate species.

dimension and at −68 ppm in the ^{29}Si dimension, consistent with interactions between the PHAPTMS silanization species and grafted T^3 sites on ZSM-5 nanocrystal exterior surfaces. The absence of correlated signal intensity between aromatic PHAPTMS protons (6.5−7.0 ppm) and Q^4 ^{29}Si sites (−110 ppm) indicates that the silanizing species are not in the vicinity of ZSM-5 framework Si species. Weak correlated signal intensity near 6.5 ppm ^{1}H and −103 ppm ^{29}Si is consistent with a fraction of the PHAPTMS species being associated with silanol moieties on the exterior nanocrystal surfaces. Based on these results, it can be concluded that the PHAPTMS surface-silanization species are not located within the zeolite nanopores but rather are grafted onto the outer surfaces of the ZSM-5 zeolite nanocrystals.

Figure 8 shows a schematic and idealized diagram that is consistent with all of the previously presented data and analyses and accounts for the different distributions of the structure-directing TPA^+ and surface-silanizing PHAPTMS species in as-synthesized ZSM-5 zeolite materials. As expected, the TPA^+ cations are located mainly within the

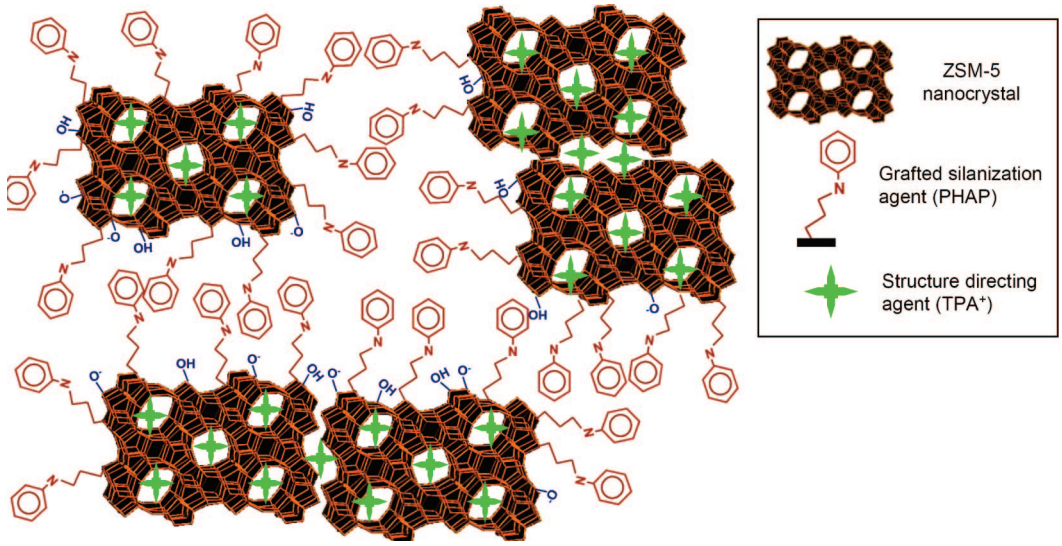

Figure 8. Schematic diagram showing the distributions of the TPA^+ zeolite-structure-directing and PHAPTMS surface-silanization species with respect to the interior nanopores and exterior surfaces of ZSM-5 zeolite nanocrystals.

zeolitic nanopores in both conventionally crystallized and nanocrystalline ZSM-5 materials, whereas the PHAPTMS seed silanization agent is distributed on the exterior surfaces of the nanocrystals. When the samples are subjected to calcination in air, both types of organic compounds are removed by oxidation, leading to the development of intracrystalline nanoporosity and interstitial mesoporosity, as detected in the adsorption isotherm measurements (Supporting Information and Table 1).

The presence of hierarchical porosity in the nanocrystalline ZSM-5 materials prepared here is expected to have a positive effect on the catalytic activity of these materials, particularly in the processing of large molecules, as it may reduce both steric and diffusional constraints on mass transfer. To test this hypothesis, several of the different ZSM-5 zeolite materials analyzed above were tested as catalysts for the cracking of low-density polyethylene (LDPE), a reaction that is sensitive to both temperature and acid strengths of the catalysts. This reaction is of technological interest, as it has been applied to the development of feedstock recycling processes of polyolefinic plastic wastes. Here, it is used as a test reaction, where the large macromolecular LDPE species (average molecular weight of 416 000 g/mol) react principally on the external surfaces of the ZSM-5 nanocrystals, because severe diffusional limitations prevent the large LDPE polymer molecules from accessing the intraparticle nanopores. When this reaction is carried out at temperatures below 400 °C, neither amorphous silica−aluminas nor ordered mesoporous materials, such as Al-MCM-41 or Al-SBA-15, present significant activity, due to their mild acidities, compared to zeolites.[62]

Table 2 summarizes the results obtained for the cracking of low-density polyethylene over different nanocrystalline ZSM-5 catalysts. As a reference, a conventional non-nanocrystalline ZSM-5 sample has also been included (crystal sizes 5−10 μm). Importantly, all of the synthesized materials exhibit a significant LDPE cracking activity, in spite of the mild reaction conditions employed (340 °C and LDPE/catalyst ratio = 100 g/g). Indeed, the reference non-nanocrystalline material needed higher temperatures (380 °C) to provide a still much lower activity. In addition to percent LDPE conversions, values for the TOF (turnover frequency: LDPE converted per unit weight of Al in the catalyst and reaction time) are also included to account for the modestly different Al contents and thus active site concentrations of the samples. Both LDPE conversion and TOF values obtained with the ZSM-5 catalysts prepared from silanized seeds are considerably superior to that of the conventional nanocrystalline ZSM-5 material (HTP-0), which has previously been reported to be an excellent catalyst for polyolefin cracking.[63] This result is attributed to improved accessibility of the LDPE molecules to the ZSM-5 acid sites, as a consequence of the higher surface areas and hierarchical porosities of the seed-silanized nanocrystalline ZSM-5 catalysts. This effect is more pronounced for the samples prepared by precrystallization at 90 °C (HTP), compared to 40 °C (LTP), suggesting that the overall acid strength of the zeolite may depend on nanocrystal size and, therefore, on the proportion of external surface area. It has been reported that the acid sites located on the external surfaces of ZSM-5 zeolite crystallites may present somewhat lower acid strengths

Table 2. Cracking of LDPE (molecular weight 416 000) over Different Nanocrystalline *n*-ZSM-5 Zeolite Catalysts[a]

sample	conversion (%)	selectivity by groups (wt %)			TOF (s^{-1})
		C_1-C_5	C_6-C_{12}	$>C_{13}$	
ZSM-5 [b]	3	100	0	0	0.018
n-ZSM-5 (LTP-5)	59	46	54	0	0.581
n-ZSM-5 (HTP-0)	36	63	37	0	0.384
n-ZSM-5 (HTP-5)	86	59	41	0	0.901
n-ZSM-5 (HTP-12)	65	58	42	0	0.726

[a] T = 340 °C; g LDPE/g catalyst = 100; time = 2 h. [b] Reference catalyst: conventional ZSM-5 zeolite, crystal size = 5−10 μm; Si/Al = 30; S_{BET} = 404 m^2/g; reaction temperature = 380 °C.

(62) Aguado, J.; Sotelo, J. L.; Serrano, D. P.; Calles, J. A.; Escola, J. M. *Energy Fuels* **1997**, *11*, 1225.

(63) Serrano, D. P.; Aguado, J.; Escola, J. M.; Garagorri, E.; Rodríguez, J. M.; Morselli, L.; Palazzi, G.; Orsi, R. *Appl. Catal. B: Env.* **2004**, *49* (4), 257.

than those in the intracrystallite nanopores.[64] Concerning selectivity of the different catalysts, for all of the materials examined, LDPE cracking leads mainly to the formation of light hydrocarbons (C_1-C_5 range) with high olefin contents, as these compounds are formed through an end-chain scission mechanism.[65] The less-acidic low-temperature precrystallized ZSM-5 product (LTP-5) yields a product distribution with a higher percentage (54 wt %) of midrange C_6-C_{12} products, although its overall activity (0.58 s^{-1} TOF, 59% conversion) is lower, compared to the otherwise identical high-temperature precrystallized ZSM-5 product (HTP-5: 41 wt % C_6-C_{12}, 0.90 s^{-1} TOF, 86% conversion). Such midrange hydrocarbons are of interest for inclusion in petrochemical feedstocks. A relatively large amount of liquid hydrocarbons is also obtained, due to the occurrence of secondary reactions that transform the light olefins into paraffins, naphthenes, and aromatic hydrocarbons. In summary, these reaction tests confirm that seed silanization syntheses of nanocrystalline ZSM-5 zeolite have significant and beneficial effects on final material properties, particularly with respect to their catalytic conversion of bulky molecules.

4. Conclusions

Silanization of protozeolitic nanoparticles has been shown to be an effective strategy for synthesizing nanocrystalline zeolite ZSM-5 with hierarchical porosity and improved catalytic reaction properties for large molecules. Such nanocrystals can be formed by the addition of a silanization agent (e.g., phenylaminopropyltrimethoxysilane, PHAPTMS) after protozeolitic nuclei have first been formed in a precrystallization step. Omitting the precrystallization treatment causes the silanization species to otherwise be only an additional silica source, hindering completely the ZSM-5 crystallization. Following grafting of the silanization species onto the exterior surfaces of protozeolitic nanoparticles, they act as a passivating layer against growth of large monolithic crystals by aggregation and fusion.

ZSM-5 zeolite products obtained from silanized seeds are comprised of aggregates of nanocrystals with sizes below 10 nm. To the best of our knowledge, this is the smallest crystal size thus far reported for ZSM-5, being close to the size of the nanoparticles that have been previously identified in the precursor solutions of MFI zeolites. However, while the latter in precursor solutions appear not to present truly crystalline features, the final nanocrystal ZSM-5 products obtained from silanized seeds exhibit clear evidence of crystallinity, namely, well defined lattice fringes and diffraction patterns in TEM and XRD measurements, despite extremely small particle sizes. Solid-state 1D and 2D NMR measurements establish that four-coordinated Al atoms are incorporated into the frameworks of as-synthesized nanocrystalline ZSM-5, that the structure-directing TPA^+ cations are located within the zeolite nanopores, and that the silanizing PHAPTMS species are located on the external surfaces of the zeolite nanocrystals.

The properties of ZSM-5 zeolite are strongly affected by the nanocrystalline character of the materials produced by seed silanization. For nanocrystalline ZSM-5 formed from silanized seeds with sizes below 10 nm, enhanced BET surface areas are measured. Moreover, these zeolites possess hierarchical porosities with subnanometer-scale pores arising from the zeolite structure and 20−30 nm mesopores arising from the interstitial voids between the nanocrystals.

The degree to which the ZSM-5 properties are modified can be controlled by altering the precrystallization conditions and the concentration of surface-silanization species used. For the conditions and compositions examined in the present study, low temperature (40 °C) precrystallization and 12 mol % of PHAPTMS relative to the silica content represent optimum conditions for the synthesis of ultrasmall ZSM-5 nanocrystals. The optimization of these variables has led to a further improvement in the textural properties compared to previous works. Thus, values of the BET surface area up to 785 m^2/g have been achieved, a significant fraction of which is contributed by the external nanoparticle surfaces. As a consequence, these materials show enhanced activity for the catalytic cracking of polyolefins, due to the large external ZSM-5 nanocrystal surface area and hierarchical porosity, which promote enhanced accessibility of large molecules to zeolite acid sites.

Acknowledgment. The Rey Juan Carlos University coauthors acknowledge financial support from "Secretaría General de Política Científica y Tecnológica, Ministerio de Educación y Ciencia" in Spain (Projects CTQ2005-09078 and CTQ2005-02375). Likewise, DPS thanks "Secretaría de Estado de Universidades e Investigación, Ministerio de Educación y Ciencia" for the fellowship received (PR2006-0078). The UCSB coauthors' contributions were supported in part by the U.S. Department of Energy, Office of Basic Energy Sciences, Catalysis Sciences DE-FG02-03ER15467, and by the USARO under Grant W911NF-05-1-0085. The NMR experiments made use of the Central Facilities of the UCSB Materials Research Laboratory supported by the MRSEC Program of the NSF under Award No. DMR 05-20415. B.F.C. thanks the Spanish Ministerio de Educación y Ciencia for fellowship support during a recent sabbatical visit.

Supporting Information Available: XRD patterns, nitrogen adsorption−desorption isotherms, FTIR spectra, and ^{27}Al and ^{29}Si MAS spectra (PDF). This material is available free of charge via the Internet at http://pubs.acs.org.

CM801951A

(64) Bevilacqua, M.; Montanari, T.; Finocchio, E.; Busca, G. *Catal. Today* **2006**, *116*, 132.
(65) Hanamura, E. *Solid State Commun.* **1987**, *63*, 1097.